Generation and Manipulation of Magnetic Droplets

Entesar ALHETLANI*, Alexander ILES, Nicole PAMME

* Corresponding author: Tel.: +44 (0) 1482 465475; Fax: +44 (0) 1482 466410; Email:
E.S.Al-Hetlani@2006.hull.ac.uk
Department of Chemistry, The University of Hull, UK

Abstract The continuous flow generation and downstream manipulation of magnetic droplets inside a microfluidic device was investigated. Magnetic droplets were generated from aqueous ferrofluids in organic oil phase using T-junction and flow-focusing geometries in glass microfluidic devices. Due to the hydrophilic nature of glass surfaces, it was necessary to apply a hydrophobic coating in the form fluorocarbons. The size of the magnetic droplets and distance between them were controlled by adjusting the relative flow velocities of ferrofluid and oil carrier liquid. Two modes of droplet manipulation were investigated by placing small permanent magnets in the vicinity of the microfluidic channels: (i) droplet deflection across a flow chamber which could be used for sorting of droplets based on the magnetic field applied and (ii) droplet splitting at a branching junction resulting in two daughter droplets of high and low magnetite content.

Keywords: Multiphase, Magnetic Droplets, Deflection, Splitting.

1. Introduction

The study of liquid droplets in microfluidic devices has recently emerged as an exciting new area. These droplets serve as nanolitre and picolitre mobile reaction vessels for numerous lab-on-a-chip applications including PCR, bioassays, protein crystallisation and nanoparticle synthesis (Song et al., 2006; Huebner et al., 2008; Teh et al., 2008). Microfluidic droplets are usually generated by merging an organic and aqueous fluid stream either at a microfluidic T-junction or at a flow focusing junction. Droplet manipulation procedures such as merging, splitting and sorting have mainly been achieved by dedicated microchannel design or by electric forces.

The magnetic manipulation of droplets can be advantageous as magnets can be easily positioned externally. Furthermore, magnetic forces are generally independent of pH and ionic strength. However, so far, droplets with magnetic functionalities have received relatively little attention. Most investigations have been conducted in open tray containers rather than microfluidic devices (Lehmann et al., 2007; Ohashi et al., 2007; Hiroyoshi et al., 2008) by pipetting a suspension of magnetic microparticles into an aqueous droplet surrounded by another immiscible phase. These magnetically functionalised droplets were then manipulated via electromagnets or permanent magnets. Reported procedures include moving droplets along the tray, merging of two droplets or splitting of droplets. Applications such as PCR or bioassays were also reported inside micro-droplets.

Here, we investigate the continuous flow generation of magnetic droplets inside microfluidic devices utilising nanoparticle suspensions (ferrofluids). Furthermore, we report on two continuous flow manipulation procedures, namely the deflection of droplets across a chamber for sorting applications and the splitting of droplets into daughter droplets of different magnetite content.

2. Experimental

2.1 Chemicals and solutions

Water based ferrofluids, EMG 507 and EMG 705, were acquired from Ferrotec (London, UK). According to the manufacturer, EMG 507 contained $0.4 - 1.1$ % of magnetite (10 nm diameter iron oxide particles) and $0.5 - 1.5$ % of anionic surfactant, whereas EMG 705

contained 1 – 4 % of magnetite and 7 – 27 % of anionic surfactant. The oil phase was obtained by mixing perfluorodecalin (Fisher Scientific) and 1H,1H,2H,2H perfluoro-1-octanol (Sigma Aldrich) at a ratio of 10 : 1 v/v. For coating of glass surfaces, 290 µL of the silanising reagent, trichloro-(perfluorooctyl)-silane (sigma Aldrich,) was dissolved in 5 mL of isooctane (Fisher scientific) and pumped manually through the microfluidic device for a period of 15 min.

2.2 Microfluidic devices and setup

Microfluidic devices were fabricated from glass via photolithography HF wet etching and thermal bonding. Two different chip designs, (A) and (B), were used for droplet deflection and droplet splitting experiments, respectively. *Droplet deflection*: Chip design (A) as shown in Fig. 1 featured a T-junction for droplet generation and a flow chamber for downstream deflection of magnetic droplets. For the T-junction, ferrofluid could be introduced through two 100 µm wide channels (only one was used here) and the oil mixture through a 150 µm wide channel. A further oil inlet fed into the 2 mm wide and 6 mm long deflection chamber. The chip was etched to a depth of 30 µm. Fused silica capillaries (150 µm i.d., Polymicro Technologies, USA) were glued to the inlet holes and connected to glass gas-tight syringes (SGE Analytical Science, Australia) via a short piece of PTFE tubing. Three syringe pumps (Harvard Apparatus, USA) were used to control the flow rates of the oil and ferrofluid independently.

To generate droplets at the T-junction, ferrofluid was pumped at 2 µL h^{-1} and the oil at 26 µL h^{-1}. The oil mixture feeding the deflection chamber was pumped at 330 µL h^{-1} (equivalent to 1.6 mm s^{-1}). For magnetically induced deflection, two different cylindrical NdFeB magnets were employed: a smaller magnet of 10 mm diameter and 3 mm thickness as well as a larger 20 mm × 5 mm magnet. These were placed on top of the deflection chamber as indicated in Fig. 1b.

Droplet splitting: Chip design (B) (Fig. 2) featured a flow focusing junction for droplet generation and a branching junction for droplet splitting. The ferrofluid inlet channel was
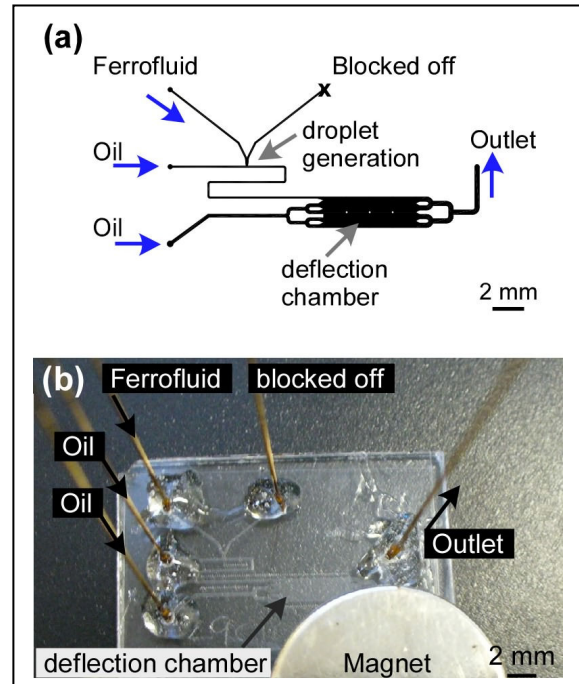

Fig. 1. Chip design (A), used for the magnetic droplet generation and downstream deflection: (a) AutoCAD drawing of the chip design showing the T-junction and the 2 mm × 6 mm deflection chamber. (b) Photograph of experimental setup with NdFeB magnet.

100 µm wide and the two surrounding oil inlet channels were 100 µm in width. The generated droplets were then pumped through a short 100 µm wide channel towards the perpendicular splitting channel, which was 50 µm in width and led towards outlet 1 and outlet 2. All channels were etched to 50 µm deep. The chip was interfaced to glass syringes as described above. Ferrofluid and oil flow were controlled independently via two syringe pumps. A variety of flow rates were investigated as indicated in the results section. For magnetically mediated droplet splitting, block NdFeB magnets (20 mm × 10 mm × 5 mm) were placed onto top of the chip as shown in Fig. 2b.

Droplets were observed using an inverted microscope (TE2000-U, Nikon, Japan) and videos were captured using a Retiga EXi digital CCD camera (QImaging, UK) with ImagePro software. Image analysis such as

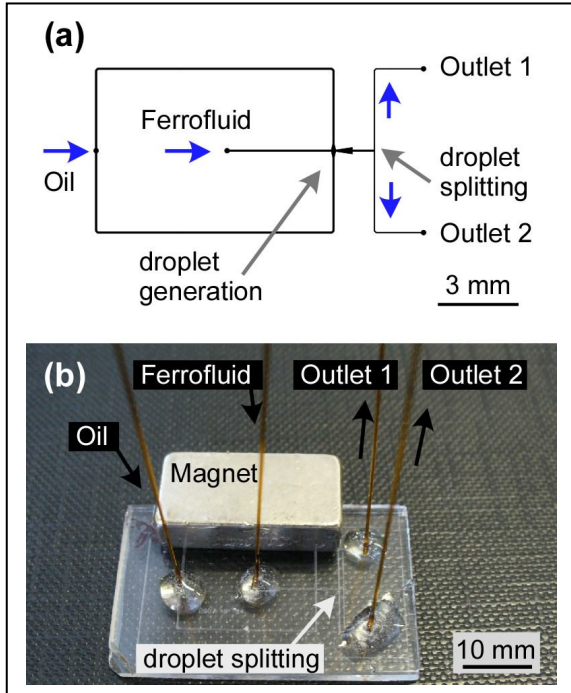droplet size measurements, greyvalue intensities and velocity measurements were carried out using ImageJ freeware (http://rsbweb.nih.gov/ij).

Fig. 2. Chip design (B), used for the generation and downstream splitting of magnetic droplets: (a) Chip design with flow focusing junction for droplet generation and branching junction towards two outlets. (b) Photograph of a typical experimental setup with block magnet.

3. Theory

3.1 Droplet deflection

The magnetic force ($\mathbf{F_{mag}}$) acting on the ferrofluid droplets in the presence of a magnetic field can be calculated according to Eq. 1 (Lehmann et al., 2007):

$$\mathbf{F_{mag}} = \frac{1}{\mu_0} \cdot \Delta\chi \cdot N \cdot V_m \cdot (\mathbf{B} \cdot \nabla)\mathbf{B} \qquad (1)$$

Where μ_0 is the permeability of free space ($4\pi \times 10^{-7}$ H m^{-1}), $\Delta\chi$ is the difference in magnetic susceptibility between the magnetic material and surrounding medium, N is the number of magnetic nanoparticles, V_m is the volume of a magnetic nanoparticle and B is the magnetic flux density.

When a droplet moves through an oil phase, as in the case of the deflection experiments, the magnetic force is opposed by an equal, but opposite drag force ($\mathbf{F_{drag}}$):

$$\mathbf{F_{drag}} = -6 \cdot \pi \cdot \eta \cdot r \cdot \mathbf{u_{mag}} \qquad (2)$$

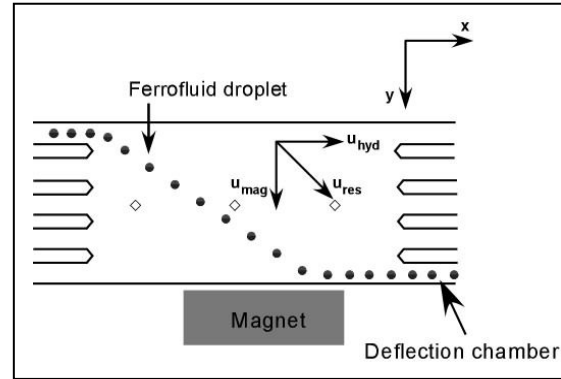Where η is the viscosity of the carrier liquid,

Fig. 3. Schematic of the magnetic droplet behaviour in a deflection chamber in the presence of the magnetic field: The magnetic droplets are deflected from the direction of the hydrodynamic flow ($\mathbf{u_{hyd}}$) in the presence of the magnetic field due to magnetically induced velocity ($\mathbf{u_{mag}}$).

r is the radius of the droplet and $\mathbf{u_{mag}}$ is the velocity of the droplet induced by the magnetic field.

Since $\mathbf{F_{mag}} = - \mathbf{F_{drag}}$, equations 1 and 2 can be combined and rearranged to give:

$$\mathbf{u_{mag}} = \left[\frac{1}{6 \cdot \pi} \frac{\Delta\chi \cdot N \cdot V_m}{\eta \cdot r} \right] \cdot \left[\frac{(\mathbf{B} \cdot \nabla)\mathbf{B}}{\mu_0} \right] = m_s \cdot S \qquad (3)$$

With m_s defined as the magnetophoretic mobility being a function of the size and magnetic loading of the droplets and S defined as the magnetophoretic driving force being a function of the strength and gradient of the applied magnetic field.

The observed deflection of the magnetic droplets in the deflection chamber depends on the magnetically induced velocity as well as the applied flow rate (Fig. 3). The velocity vector of the applied hydrodynamic flow ($\mathbf{u_{hyd}}$) is in the x-direction, whereas the vector of the magnetically induced velocity ($\mathbf{u_{mag}}$) acts predominantly in the y-direction. The observed droplet trajectory is the sum of these two vectors $\mathbf{u_{res}}$:

$$\mathbf{u_{res}} = \mathbf{u_{hyd}} + \mathbf{u_{mag}} \qquad (4)$$

3.2 Droplet splitting

Droplet splitting at a perpendicular

junction was first described by Song et al., 2003. The process of splitting proceeds through two steps: (i) droplet deformation followed by (ii) droplet breakup. As the droplet is pressed against the branching point, sheer forces dominate and the droplet is split into two equally sized daughter droplets. The size of the daughter droplet can be varied by changing the relative size of the branching channel or by applying different pressures to the two outlets.

4. Results and discussion

4.1 Droplet deflection experiments

Magnetic droplets were deflected using chip design (A) as indicated in the experimental section. In Fig. 4, the generation of ferrofluid droplets at the T-junction is shown. The ferrofluid stream was seen to break up at the junction into droplets of 155 ± 12 µm in diameter and dispersed in the oil.
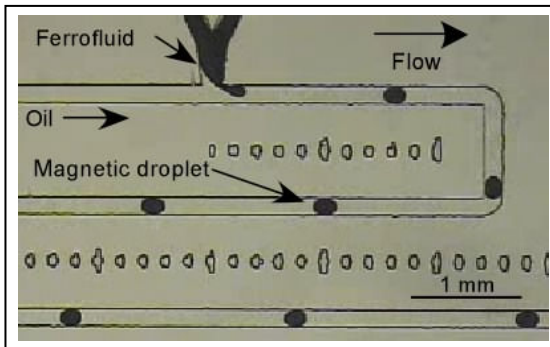

Fig. 4. Magnetic droplets generated utilising chip design (A) in continuous flow using a T-junction. The oil was pumped at 26 µL h^{-1} and the ferrofluid at 2 µL h^{-1}.

When the droplets were introduced into the deflection chamber, they followed the laminar flow in the x-direction and passed straight through the chamber leaving via the exit opposite the droplet inlet (Fig. 5a). When a magnetic field was applied, the droplet behaviour changed (Fig. 5b, c). The magnetic droplets were attracted to the magnetic field and thus deflected from the direction of flow to leave the chip via different exits. The extent of deflection was investigated with two different magnets placed at the same position

on the deflection chamber. When the smaller NdFeB magnet (10 mm × 3 mm) was used, the droplets were observed to leave via exit 2 (Fig. 5b). The magnetic force acting on the droplets was calculated according to Eq. (6), and estimated to be 5.5 ± 0.4 nN.

When using the larger NdFeB magnet (20 mm × 5 mm), the same droplets were pulled further and all left via exit 3 (fig. 5c). The magnetic force, increased by the larger magnetic field strength and gradient, was estimated to be 8.5 ± 1.6 nN. Deflection across the flow chamber could be used for guiding droplets towards different outlets as desired for particular downstream applications.
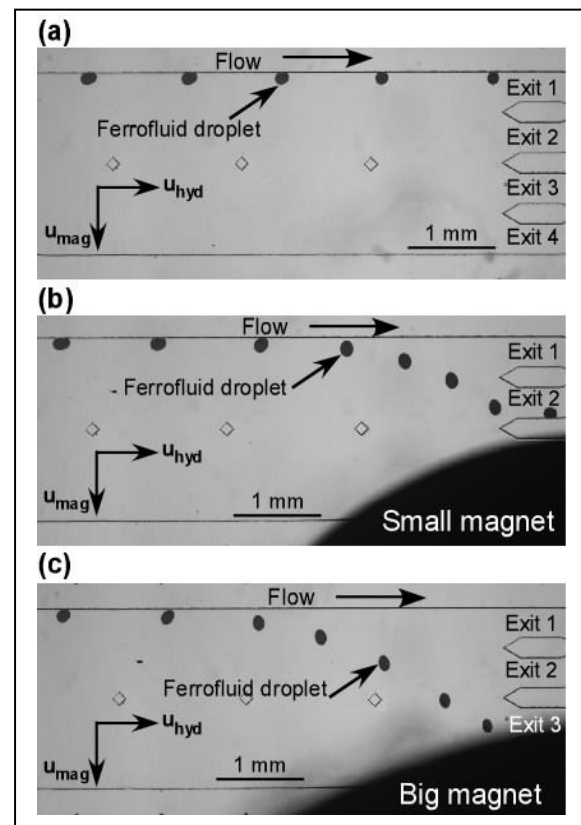

Fig. 5. Droplets moving in the deflection chamber part of the chip (a) the magnetic droplets in the deflection chamber in the absence of the magnetic field moving in a straight path leaving via exit 1. (b) In the presence of the small magnet droplets start to deflect and leave via exit 2. (c) In the presence of the big magnet the droplets start to deflect and leave via exit 3.

4.2 Droplet splitting experiments

The magnetic droplets generation and splitting was investigated using chip design (B) as described in the experimental section.

In Fig. 6a, the generation of ferrofluid droplets and downstream splitting is shown in the absence of a magnetic field. Ferrofluid was pumped at $0.7 \ \mu L \ min^{-1}$ and the oil mixture was pumped at $5 \ \mu L \ min^{-1}$. The droplets formed were $153 \pm 24 \ \mu m$ in diameter. At the splitting junction, the droplets were deformed and split into two identical daughter droplets.
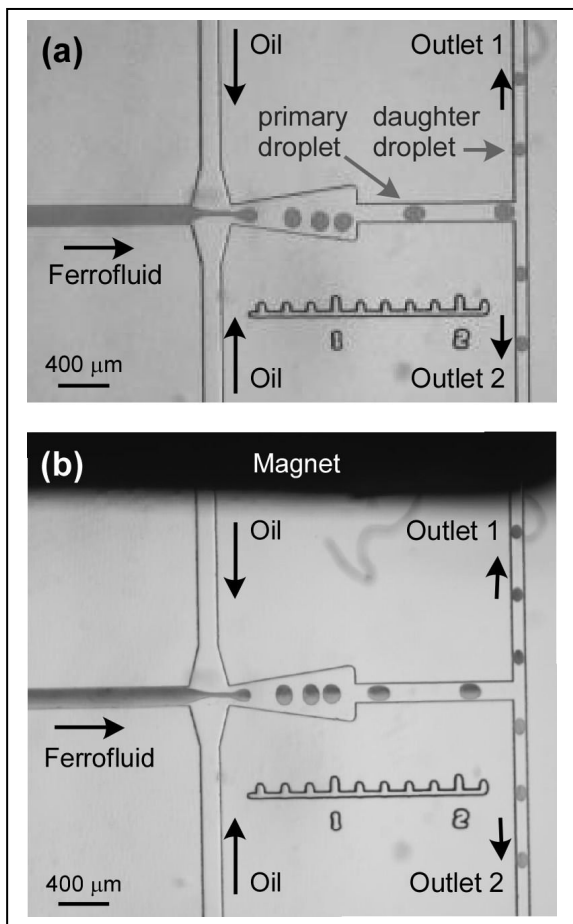

Fig. 6. Flow focusing chip design used to generate the magnetic droplets. (a) Droplets generated without the magnet present. (b) Droplets generated in the presence of the magnet and split into two magnetic and non-magnetic droplets.

The area of the mother droplet was measured using ImageJ and found to be $2 \times 10^4 \pm 9 \times 10^2 \ \mu m^2$ and the daughter droplet was $9.9 \times 10^3 \pm 1.1 \times 10^3 \ \mu m^2$. This indicated that the mother droplet split to produce two daughter droplets that were half its size.

When a magnetic field was applied, the iron oxide nanoparticles in the ferrofluid were attracted towards the magnet and accumulated in one half of the droplet (Fig. 6b). At the

splitting junction, droplets flowing into outlet 1 were enriched in magnetite whereas droplets flowing into outlet 2 were depleted.

The magnetic content of the daughter droplets was quantified by measuring the greyvalue for both types of droplets: the darker the droplet, the higher its magnetic content and the higher its grey value. The obtained data is presented in Fig. 7. It can be clearly seen that the enriched droplets feature a greatly enhanced grey scale value. Data was taken from droplets generated at different ferrofluid flow rates $0.3 - 1 \ \mu L \ min^{-1}$. The variation in flow rate did not affect the efficiency of magnetite enrichment and depletion. Fig. 7 represents the data collected at the highest ferrofluid flow rate used in the splitting experiment ($1 \ \mu L \ min^{-1}$).
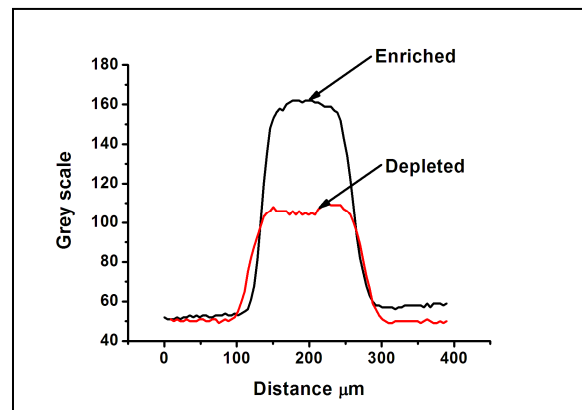

Fig 7. Optical density analysis results: a plot of the grey value versus droplet diameter shows the different results for the droplets. The non magnetic droplets have a low grey value in comparison to the grey value for the droplet nearest to the magnet.

Magnetic depletion and enrichment could be used as part of a digital microfluidic system in which magnetic functionality can be added and removed as required. In contrast to the deflection experiments in the 1.6 mm wide deflection chamber, the droplets here were constrained by the 100 μm wide channel and the interaction with the magnetic field was limited to the attraction of the nanoparticles in the ferrofluid. In addition, the applied flow velocities were high in the splitting experiments, $17 \ mm \ s^{-1}$ compared to $1.6 \ mm \ s^{-1}$ used for deflection experiments. Hence, droplets were subjected to high $\mathbf{u}_{mag}$ values (Eq. 4) in the deflection work.

5. Conclusion

The continuous flow generation and manipulation of magnetic droplets was demonstrated in microfluidic devices.

Magnetic droplets were generated in continuous flow using different chip designs. In one setup, droplets were generated at a T-junction and then introduced into a 2 mm wide flow chamber. When a magnetic field was applied, droplets were deflected from the direction of flow depending on the strength of the field. In a second series of experiments, droplets were generated at a flow focusing junction and split downstream into daughter droplets of differing magnetite content. By applying a magnetic field, droplets were enriched and depleted in magnetite.

We have thus demonstrated the continuous flow of magnetic manipulation of droplets as a feasible method for operations including splitting and sorting. Future studies will be aimed at further elucidating parameters affecting droplet deflection and splitting and finally utilising the magnetic functionality for an analytical application.

Acknowledgements

6. References

Hiroyoshi, T., Mina, O., Nobuhiro, N., Mitsuhiro, S., Hiroyuki, H., 2008. On-chip polymerase chain reaction microdevice employing a magnetic droplet- manipulation system. Sens. Act. B. 130, 583-588.

Huebner, A., Sharma, S., Srisa-Art, M., Hollfelder, F., Edel, J., deMello, A., 2008. Microdroplets: A sea of applications?, Lab Chip. 8, 1244–1254.

Lehmann, U., de Courten, D., Vandevyver, C., Parashar, V., Gijs, M., 2007. On-chip antibody handling and colorimetric detection in a magnetic droplet manipulation system. J. Microelec. Eng. 84, 1669–1672.

Ohashi, T., Kuyama, H., Hanafusa, N., Togawa, Y., 2007. A simple device using magnetic transportation for droplet-based PCR. Biomed. Microdev. 9, 695-702.

Song, H., Chen, D., Ismagilov, R., 2006. Reactions in Droplets in Microfluidic Channels. Angew Chem Int Ed Engl. 45, 7336-7356.

Song, H., Tice, J., Ismagilov, R., 2003. A microfluidic system for controlling reaction networks in time. Angew. Chem. Int. Ed. 42, 768-772.

Teh, S., Lin, R., Hung, L., Lee, A., 2008. Droplet microfluidics. Lab Chip. 8,198 - 220.

Zheng, B., Tice, J., Ismagilov, R., 2004. Formation of droplets of alternating composition in microfluidic channels and applications to indexing of concentrations in droplet-based assays. Anal. Chem. 76, 4977-4982.